THE JOURNAL OF BIOLOGICAL CHEMISTRY VOL. 286, NO. 15, pp. 13143–13150, April 15, 2011

Functional Reconstitution of an Atypical G Protein Heterotrimer and Regulator of G Protein Signaling Protein (RGS1) from *Arabidopsis thaliana*[*]

Received for publication, September 30, 2010, and in revised form, February 1, 2011 Published, JBC Papers in Press, February 16, 2011, DOI 10.1074/jbc.M110.190355

Janice C. Jones[‡1], **Brenda R. S. Temple**[‡§], **Alan M. Jones**[¶‖2], **and Henrik G. Dohlman**[‡¶3]

From the [‡]*Department of Biochemistry and Biophysics,* [§]*R. L. Juliano Structural Bioinformatics Core Facility, and Departments of* [¶]*Pharmacology and* [‖]*Biology, University of North Carolina at Chapel Hill, Chapel Hill, North Carolina 27599*

It has long been known that animal heterotrimeric G$\alpha\beta\gamma$ proteins are activated by cell-surface receptors that promote GTP binding to the Gα subunit and dissociation of the heterotrimer. In contrast, the Gα protein from *Arabidopsis thaliana* (AtGPA1) can activate itself without a receptor or other exchange factor. It is unknown how AtGPA1 is regulated by G$\beta\gamma$ and the RGS (regulator of G protein signaling) protein AtRGS1, which is comprised of an RGS domain fused to a receptor-like domain. To better understand the cycle of G protein activation and inactivation in plants, we purified and reconstituted AtGPA1, full-length AtRGS1, and two putative G$\beta\gamma$ dimers. We show that the *Arabidopsis* Gα protein binds to its cognate G$\beta\gamma$ dimer directly and in a nucleotide-dependent manner. Although animal G$\beta\gamma$ dimers inhibit GTP binding to the Gα subunit, AtGPA1 retains fast activation in the presence of its cognate G$\beta\gamma$ dimer. We show further that the full-length AtRGS1 protein accelerates GTP hydrolysis and thereby counteracts the fast nucleotide exchange rate of AtGPA1. Finally, we show that AtGPA1 is less stable in complex with GDP than in complex with GTP or the G$\beta\gamma$ dimer. Molecular dynamics simulations and biophysical studies reveal that altered stability is likely due to increased dynamic motion in the N-terminal α-helix and Switch II of AtGPA1. Thus, despite profound differences in the mechanisms of activation, the *Arabidopsis* G protein is readily inactivated by its cognate RGS protein and forms a stable, GDP-bound, heterotrimeric complex similar to that found in animals.

Heterotrimeric G proteins are activated by cell-surface G protein-coupled receptors (GPCRs)[4] in response to extracellular stimuli. Typically, an extracellular ligand binds to and activates a GPCR, which in turn promotes guanine nucleotide exchange by the α-subunit of the G$\alpha\beta\gamma$ protein heterotrimer. Gα-GTP binding results in heterotrimer dissociation *in vitro*, although some heterotrimers appear to remain associated *in vivo* (1, 2). Activated Gα proteins and free G$\beta\gamma$ dimers act on downstream effector enzymes to initiate a cellular response to the stimulus. Signaling is terminated after the Gα subunit hydrolyzes GTP to GDP and reassociates into the resting heterotrimeric complex. Regulators of G protein signaling (RGS) proteins promote signal termination by accelerating the GTPase activity of the Gα subunit. These signaling components are found throughout all eukaryotes where they respond to a variety of stimuli including light, hormones, pheromones, and neurotransmitters (reviewed in Refs. 3 and 4).

Recently, exceptions to the G protein signaling paradigm were discovered in the plant model organism *Arabidopsis thaliana*. Whereas animal Gα proteins have a slow rate of nucleotide exchange in the absence of an activated GPCR or other guanine nucleotide exchange factor, the *Arabidopsis* Gα (AtGPA1, herein referred to as GPA1) rapidly releases GDP without any stimulus (5). In fact, the rate of GPA1 nucleotide exchange is >100-fold faster than its rate of GTP hydrolysis, suggesting that this Gα protein would be almost entirely GTP-bound in a cell where GTP is in excess over GDP. However, GTPase-deficient GPA1 confers distinct cell proliferation phenotypes in plants (6, 7), indicating that additional components maintain a portion of GPA1 in an inactive state *in vivo*.

GPA1 shares limited sequence similarity with its animal counterparts (38% identical, 56% similar to $G\alpha_{i1}$). In addition to a divergent Gα protein, *Arabidopsis* has an RGS protein with an unusual domain architecture. Whereas most animal RGS proteins are present in the cytoplasm, the RGS protein from *Arabidopsis* is fused to a predicted seven-transmembrane domain reminiscent of GPCRs and localizes to the plasma membrane (7). The atypical nature of these signaling components suggests that some plants employ a signaling mechanism distinct from that found in animals or fungi. Here, we investigate the mechanisms of G protein regulation in *Arabidopsis*, with a particular focus on G$\beta\gamma$ and full-length RGS1.

[*] This work was supported, in whole or in part, by National Institutes of Health Grants GM080739 and GM082892 (to H. G. D.) and GM065989 (to A. M. J.) from the NIGMS. This work was also supported by Department of Energy Grant DE-FG02-05er15671 and National Science Foundation Grants MCB-0723515 and MCB-0718202 (to A. M. J.).

[1] Supported by a Ruth Kirchstein F32 postdoctoral award.

[2] To whom correspondence may be addressed: Dept. of Biology, CB 3280, Chapel Hill, NC 27599. Tel.: 919-962-6932; E-mail: alan_jones@unc.edu.

[3] To whom correspondence may be addressed: Dept. of Biochemistry and Biophysics, CB 7260, Chapel Hill, NC 27599. Tel.: 919-843-6894; E-mail: henrik_dohlman@med.unc.edu.

[4] The abbreviations used are: GPCR, G protein-coupled receptor; AGB1, *Arabidopsis* G β-subunit 1; AGG1, *Arabidopsis* G γ-subunit 1; AGG2, *Arabidopsis* G γ-subunit 2; GAP, GTPase accelerating protein; GMPPNP, guanosine 5′-[β,γ-imido]triphosphate (nonhydrolyzable GTP analog); GTPγS, guanosine 5′-O-[gamma-thio]triphosphate (nonhydrolyzable GTP analog); MANT, *N*-methylanthraniloyl fluorophore; MD, molecular dynamics; RGS, regulator of G protein signaling.

Animal Gβγ dimers diminish G protein activation by acting as a guanine nucleotide dissociation inhibitor to prevent spontaneous GDP release from Gα proteins and thereby help maintain the inactive state (8). *Arabidopsis* has a single Gβ protein (AGB1) (9) and at least two Gγ proteins (AGG1 and AGG2) (10–12). AGB1 is 64% similar to human Gβ2, and the two *Arabidopsis* Gγ proteins lack significant similarity to their animal counterparts, although residues critical for Gγ function are conserved (11, 12). Moreover, it has been shown that plant G protein heterotrimeric components associate as a part of a large undefined macromolecular complex *in vivo* even when the Gα protein is activated by GTP (1, 13). Direct interaction between G protein subunits has not been shown previously with purified components, and possible guanine nucleotide dissociation inhibitor activity of plant Gβγ proteins toward GPA1 had not been investigated; thus, it is not known whether GPA1 retains its self-activation property within the heterotrimeric complex.

The unusual features of the *Arabidopsis* G protein signaling components prompted us to investigate their properties biochemically. Using purified heterotrimer and full-length RGS1 protein, we established conditions that either promote or disrupt heterotrimer association, we measured the effect of the two plant Gβγ dimers on GPA1 activity, and we showed that the full-length RGS1 protein serves to counteract the rapid rate of nucleotide exchange by GPA1 and impose the inactive conformation of this Gα protein. Furthermore, we showed that GPA1 is most stable as a Gα-GDP-Gβγ complex or in the Gα-GTP state, but relatively unstable as a Gα-GDP complex. Finally, we used computational methods to identify possible determinants of the relative instability of the Gα-GDP complex and tested these predictions with biophysical methods. Together, our results reveal the characteristics of this plant G protein signaling module, representing an informative counterexample to the well established paradigm for G protein signaling in animals.

EXPERIMENTAL PROCEDURES

Gα Protein Purification—Hexahistidine-tagged GPA1 and $G\alpha_{i1}$ were purified from *Escherichia coli* Codon Plus DE3 BL21 RIPL cells (Stratagene) as described before for GPA1 (14). The Q222L mutation was introduced into GPA1 with the QuikChange site-directed mutagenesis kit (Stratagene), and the mutant protein was purified by the same method as the wild-type protein.

Gβγ Protein Purification—AGG1 or AGG2 with an N-terminal hexahistidine tag and a CAA*X*-to-SAA*X* mutation (to decrease membrane localization) were subcloned into the pFastBacDual vector (Invitrogen) with AGB1 for expression in Sf9 cells with the baculovirus expression system. These proteins were expressed from a P3 virus with an approximate multiplicity of infection of 1 for 60 h for AGB1/AGG1 or 48 h for AGB1/AGG2. Cell pellets were resuspended in ice-cold lysis buffer (25 mM Tris, pH 8, 200 mM NaCl, 20 mM imidazole, 1 mM 2-mercaptoethanol, protease inhibitor mixture), and cells were disrupted with three passes through an EmulsiFlex homogenizer (Avestin). Cells were then dounce homogenized five times, and debris was collected by ultracentrifugation at 50,000 × *g* for 30 min at 4 °C. The ultracentrifugation supernatant was incubated with 1 ml of nickel-nitrilotriacetic acid beads (GE Healthcare) for ~1 h at 4 °C. Beads were washed with lysis buffer (without 2-mercaptoethanol) until the protein was no longer detectable in washes (as determined by a Bio-Rad protein assay reagent). AGB1/AGG1 or AGB1/AGG2 was eluted with lysis buffer (plus 20% glycerol v/v and 250 mM imidazole). Peak elution fractions from the nickel column were identified by SDS-PAGE analysis and loaded onto an S200 size exclusion column. Peak S200 fractions were pooled and concentrated with a spin concentrator (Viva Science) and flash-frozen in liquid nitrogen. $G\beta_1\gamma_2$ was a gift from Janeen Vanhooke in the laboratory of John Sondek (University of North Carolina, Chapel Hill).

Expression of Full-length RGS1 in Sf9 Cells—Full-length *Arabidopsis* RGS1 with a C-terminal hexahistidine tag was expressed in *Sf9* cells from a P3 virus with a multiplicity of infection of ~1 for 60 h. Cell pellets were lysed in SF9B (50 mM Tris, pH 7.4, 100 mM NaCl, 1 mM $MgCl_2$, protease inhibitor mixture) with an EmulsiFlex homogenizer. Cell debris was removed by low speed centrifugation (1000 × *g* for 10 min at 4 °C). To collect membranes, the supernatant from the low speed spin was subjected to ultracentrifugation (200,000 × *g* for 1 h at 4 °C). Transparent pellets from ultracentrifugation were resuspended in SF9B. RGS1 was greatly enriched in these crude membrane preparations as detected by Western blot against the hexahistidine tag. The purified RGS box protein was a gift from Adam Kimple in the laboratory of David Siderovski (University of North Carolina, Chapel Hill) and Tyrell Carr in the laboratory of Alan Jones.

Size-exclusion Chromatography of G Protein Heterotrimeric Complexes—Purified Gα protein (50–100 μg, final concentration of 5–9 μM) in 150 μl SDB (20 mM Tris, pH 8, 50 mM NaCl, 1 mM EDTA, 2 mM $MgCl_2$, 1 mM DTT) or a control buffer was incubated with GDP (25 μM), GTPγS (25 μM), or GDP-AF (25 μM GDP, 20 mM NaF, 30 μM $AlCl_3$) for 15 min at room temperature. The Gβγ dimer (50–70 μg, final concentration of 4–6 μM) or a control buffer was added, and the mixture was incubated for an additional 20 min at room temperature. The entire mixture (250 μl) was loaded onto a 1-ml superloop, chased with 500 μl of SDB (with 10 μM nucleotide), and injected onto a Superdex 200 FPLC size-exclusion column. The column was developed with SDB (with 10 μM nucleotide) as A_{280} was monitored. Elution fractions were analyzed by SDS-PAGE analysis.

Measurement of Steady-state GTP Hydrolysis and ^{32}P Occupancy of GPA1—Purified GPA1 (250 nM) in HEL buffer (20 mM HEPES, pH 7, 1 mM EDTA, 0.1% Lubrol (v/v)) was mixed with an RGS box (residues 249–459, 500 nM) or a control buffer before the reaction was started by adding $MgCl_2$ (5 mM), [γ-^{32}P]GTP (~5000–10,000 cpm/pmol), and GTP (2.5 μM). At the indicated time point, samples were quenched into 3 ml of ice-cold WB buffer (20 mM Tris, pH 7.4, 100 mM NaCl, 25 mM $MgCl_2$) and rapidly filtered through nitrocellulose. Filters were washed once with ice-cold WB buffer and scintillation-counted to determine the fraction of GPA1 bound to ^{32}P. Twenty min after the start of the reaction, a large excess of nonradioactive GTPγS (100 μM) was added to the reaction to prevent further [γ-^{32}P]GTP loading. For experiments with full-length RGS1, purified GPA1 (wild-type or Q222L, 275 nM) was mixed with

crude membrane preparations containing RGS1 before starting the reaction by adding $MgCl_2$ (10 mM), [γ-^{32}P]GTP (~1000 cpm/pmol), and GTP (10 μM). At the given time point, the reaction was stopped by quenching in HPO_4 buffer, pH 2, with 5% charcoal (w/v). After quenching and charcoal extraction, which denatures proteins and removes organic compounds, supernatants were Cherenkov-counted to quantify the GTP hydrolyzed. Experiments with G$\beta\gamma$ protein were done in a similar manner as with full-length RGS1 protein except that samples labeled with "0 °C" were incubated on ice for 1 h before starting the reaction at time 0 by adding [γ-^{32}P]GTP and $MgCl_2$. Samples labeled with "23 °C" were incubated on ice for 30 min then moved to room temperature for 30 min before starting the hydrolysis reaction. Where indicated, AGB1/AGG1 or AGB1/AGG2 was added 1 h prior to starting the hydrolysis reaction.

Measurement of G Protein Inactivation by RGS Box with Intrinsic Fluorescence—Intrinsic fluorescence (excitation, 284 nm; emission, 340 nm) of GPA1 (300 nM) with or without RGS box protein (600 nM) was measured after the addition of GTP (300 nM). GTPγS (2 μM) was added to the RGS-containing sample where indicated with an arrow to confirm that GPA1 was active in this reaction. Data shown for one experiment are representative of three individual experiments.

Measurement of Nucleotide Binding by MANT Fluorescence—MANT-GDP or MANT-GMPPNP (400 nM) was equilibrated in a cuvette with 1 ml TENG buffer (25 mM Tris, pH 8, 1 mM EDTA, 100 mM NaCl, 5% v/v glycerol) and 5 mM $MgCl_2$ where indicated. To measure nucleotide association, purified GPA1 (300 nM) was added to the equilibrated MANT nucleotide, and the increase in MANT fluorescence (excitation, 360 nm; emission, 440 nm) was monitored over time. Where indicated, AGB1/AGG1 (1250 nM) was incubated with GPA1 for 30 min at room temperature before adding the mixture to the cuvette.

Measurement of Single Turnover GTP Hydrolysis with AGB1/AGG1—Gα protein (250 nM) in HEL buffer with 0.5 mM $MgCl_2$ was incubated with [γ-^{32}P]GTP for 5–10 min at room temperature to allow [γ-^{32}P]GTP-loaded GPA1 to accumulate. A large excess of nonradioactive GTPγS (100 μM) was added when the reaction was initiated to prevent GPA1 from reloading with [γ-^{32}P]GTP, therefore limiting observed [γ-^{32}P]GTP hydrolysis to a single turnover. At the indicated time point, duplicate aliquots were quenched in HPO_4 buffer, pH 2, with 5% charcoal (w/v), and charcoal-extracted supernatants were Cherenkov-counted. The zero time point was subtracted as background hydrolysis that occurs during GTP loading. Where indicated AGB1/AGG1 or AGB1/AGG2 were preincubated with GPA1 before initiating the hydrolysis reaction.

Measurement of Protein Stability by Quantitative Cysteine Reactivity Labeling and Circular Dichroism (CD) Spectroscopy—Quantitative cysteine reactivity labeling was conducted essentially as described previously (15). GPA1 (1 μM) was incubated with GDP or GTPγS (33 μM) for 5 min at room temperature in 25 mM PO_4 buffer, pH 7, with 100 mM KCl and 2 mM $MgCl_2$ before (tris(2-carboxyethyl)phosphine) (50 μM) and (4-aminosulfonyl)-7-fluoro-2,1,3-benzoxadiazole (TCI America) (1 mM) was added to the mixture. Samples were incubated at temperatures ranging from 25 to 75 °C for 5 min in a thermocycler before the reaction was quenched with HCl (final concentration of 0.2 N). (4-Aminosulfonyl)-7-fluoro-2,1,3-benzoxadiazole fluorescence (excitation at 400 nm and emission at 500 nm) was measured for each sample, and the percent maximum GPA1 labeling was calculated by dividing the fluorescence units of each sample by the maximum fluorescence observed within the experiment. CD spectroscopy was conducted as described (16).

Molecular Modeling and Molecular Dynamics Simulations—GPA1-GDP was modeled from the structure of GPA1-GTPγS (Protein Data Bank code 2XTZ (16)) using Modeler software (17). Switch regions for the inactive conformation (GDP-bound) were modeled from the structure of $G\alpha_{i1}$ in heterotrimeric complex (Protein Data Bank code 1GP2; Ref. 18). Homology models for AGB1 and AGG1 were generated as described previously (6), and the GPA1-GDP-AGB1/AGG1 heterotrimeric complex was assembled by superimposition on 1GP2 coordinates with the PyMOL Molecular Graphics System. Molecular dynamics (MD) simulations using the Amber software suite (version 10.0) were conducted with GPA1-GDP, GPA1Δ36-GDP, GPA1Δ36-GTP, and GPA1-GDP-AGB1/AGG1 essentially as described previously (19, 20). Hydrogen atoms were added, electrostatic charge of the system was neutralized with counter ions, and proteins were solvated using 15,000–28,000 transferable interaction potential three-point water molecules as described previously (20). All MD simulations were conducted for 20 ns with a 2-fs time step using the AMBER 2003 force field (21). Root mean square fluctuations were calculated about an average structure.

RESULTS

Direct, Nucleotide-dependent Association of Arabidopsis Heterotrimer Subunits—G protein subunits typically associate into the heterotrimeric complex in the presence of GDP and dissociate in the presence of GTP. The fast spontaneous GTP binding property of GPA1 prompted us to determine whether this Gα protein can, under any circumstances, accumulate in an inactive conformation and bind directly to its cognate G$\beta\gamma$ dimer. To this end, we purified GPA1 from *E. coli* as described previously (14) as well as soluble G$\beta\gamma$ dimers (AGB1/AGG1 and AGB1/AGG2) from insect cells (see "Experimental Procedures"). We then loaded GPA1 with GDP or activating ligands (GTPγS or GDP-AlF_4^-) before addition of the AGB1/AGG1 dimer. GTPγS is a nonhydrolyzable analog of GTP, and AlF_4^- imposes the Gα conformation similar to the transition state for GTP hydrolysis (22). Next, proteins were resolved by size-exclusion chromatography and analyzed by absorbance at 280 nm and SDS-PAGE. Although G$\beta\gamma$ dimers were purified using the hexahistidine-tagged Gγ subunit, only the purified Gβ subunit is sufficiently large to be visible in our Coomassie-stained gels. In the presence of nonhydrolyzable GTP (GTPγS), GPA1 and AGB1 migrate as individual dissociated proteins (Fig. 1*A*). However, in the presence of GDP, GPA1 and AGB1 co-migrate at the faster mobility expected for a heterotrimeric complex (Fig. 1*B*). We found that the plant G$\beta\gamma$ dimer also interacts with human $G\alpha_{i1}$ in the presence of GDP (Fig. 1*C*). This heterotrimeric complex is disrupted by the activating ligand, AlF_4^- (Fig. 1*C*). We were unable to detect interaction

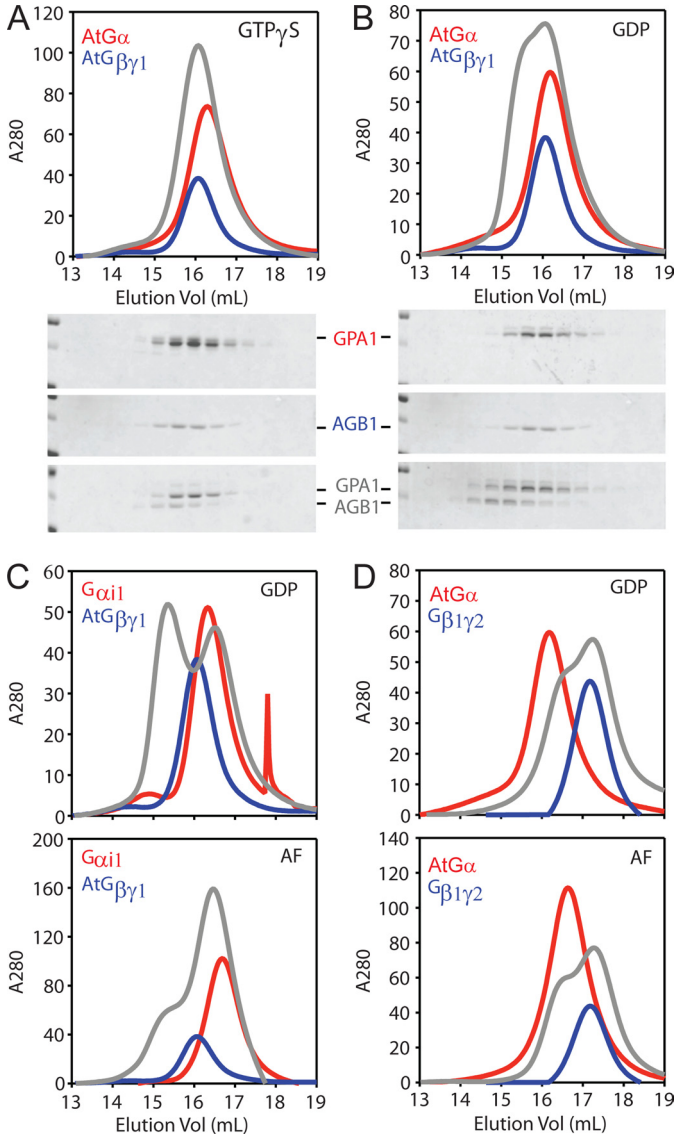

FIGURE 1. **Purification of *Arabidopsis* heterotrimeric G protein complexes.** Purified Gα protein (100 μg) or a control buffer was incubated with the indicated guanine nucleotide (20 μM) before adding purified Gβγ protein (100 μg) or a control buffer. Samples were analyzed with a Superdex 200 size-exclusion FPLC column. Protein content was monitored by absorbance at 280 nm, and fractions were analyzed by SDS-PAGE. Note that buffer contained GDP for all samples with only Gβγ. For all panels, *red lines* trace the absorbance of Gα protein alone; *blue lines* trace the Gβγ dimer alone; and *gray lines* trace the Gα and Gβγ proteins together. *A*, chromatogram and Coomassie-stained gels for GPA1 (AtGα) and AGB1/AGG1 (Gβγ1) with GTPγS. *B*, same as *A* but with GDP. *C*, chromatogram for $G\alpha_{i1}$ and AGB1/AGG1 with GDP or GDP-AlF_4^-. *D*, chromatogram for GPA1 and human $G\beta_1\gamma_2$ with GDP or GDP-AlF_4^- *(AF)*. *Vol*, volume.

between GPA1 and human $G\beta_1\gamma_2$ under any condition (Fig. 1*D*). Together, these data show that the *Arabidopsis* Gα, similar to its animal counterparts, binds directly to its cognate Gβγ dimer in the presence of GDP and that the subunits dissociate in the presence of activating ligands. Moreover, these results suggest that structural requisites for Gβ interaction with Gα proteins are conserved between *Arabidopsis* and human Gβ proteins.

GPA1 Inactivation by RGS1—GPA1 exhibits an unusually fast spontaneous rate of GDP release/GTP binding (5), suggesting that this Gα protein might not accumulate in the inactive state in a cell where GTP is in large excess over GDP. Having determined that GTP-bound GPA1 dissociates from the Gβγ dimer, we sought to identify conditions where GPA1 would assume the inactive conformation in a cell. In particular, we examined whether RGS1 is sufficient to counteract the rapid GTP binding property of GPA1. RGS proteins are known to inactivate Gα proteins by accelerating GTP hydrolysis (23). Previously, it was shown that the RGS core domain ("RGS box" residues 249–459) from the *Arabidopsis* RGS1 protein can accelerate GTP hydrolysis by GPA1 (5, 7). To determine how RGS1 affects GPA1 nucleotide occupancy, we used a radioligand binding assay to measure GTP bound to GPA1 with or without the RGS box. For this experiment, GPA1 binding to ^{32}P was measured over time after incubation with a large excess of [γ-^{32}P]GTP (radiolabeled at the γ-phosphate). Here, we found that GPA1 is ~75% activated in the absence of the RGS box (Fig. 2*A*) as expected for a G protein with fast GTP binding and slow GTP hydrolysis. In contrast, GPA1 is only ~20% activated in the presence of the RGS box (Fig. 2*A*). As a second measure of GPA1 activity, we monitored protein conformation in a fluorescence-based assay. The intrinsic fluorescence of active GTP-bound GPA1 is higher than the fluorescence of the inactive GDP-bound conformation (24, 25). Here, we found that GPA1 does not adopt an active conformation in the presence of RGS box and excess GTP (Fig. 2*B*). As a control, we show that GPA1 adopts an active conformation in the presence of the RGS box and non-hydrolyzable GTP analog, GTPγS (Fig. 2*B*, *arrow*). The RGS box does not affect the rate of binding of GTPγS (Fig. 2*B* and data not shown). Together, these results show that the GTPase accelerating activity of the RGS box of RGS1 is sufficient to counteract the self-activation property of GPA1 and impose the inactive Gα conformation.

RGS1 is a unique structural hybrid of a transmembrane receptor and an RGS protein (7). The GTPase-accelerating activity of an RGS1 fragment (RGS box, without the receptor domain) has been measured previously (5, 7). To determine whether the full-length RGS1 protein has GTPase accelerating (GAP) activity toward GPA1, we expressed RGS1 with the baculovirus expression system and isolated RGS1-containing membrane preparations from these cells. For GPA1, GTP hydrolysis is the slowest step in the nucleotide cycle; therefore, GAP activity can be determined by measuring sequential rounds of [γ-^{32}P]GTP binding and hydrolysis (5). We found that full-length RGS1 accelerates GPA1 GTP hydrolysis 15-fold from 0.076/min to 1.1/min (Fig. 2*C*). Together, these results show that full-length RGS1 can inactivate GPA1 and promote conditions for heterotrimer formation. Despite the presence of a receptor-like domain, RGS1 is functional as a GAP in the absence of any ligand.

GPA1 Self-activation in Presence of Gβγ—Within heterotrimeric complexes, mammalian Gβγ dimers are widely known to diminish Gα activation and do so by increasing GDP association and decreasing GDP dissociation (*i.e.* by functioning as guanine nucleotide dissociation inhibitors). Generally speaking, the effect of Gβγ on Gα affinity for GDP ranges from ~10- to 300-fold *in vitro*, and this guanine nucleotide dissociation inhibitor effect is diminished in animals by magnesium, which chelates the β- and γ-phosphates of GTP (8). To determine

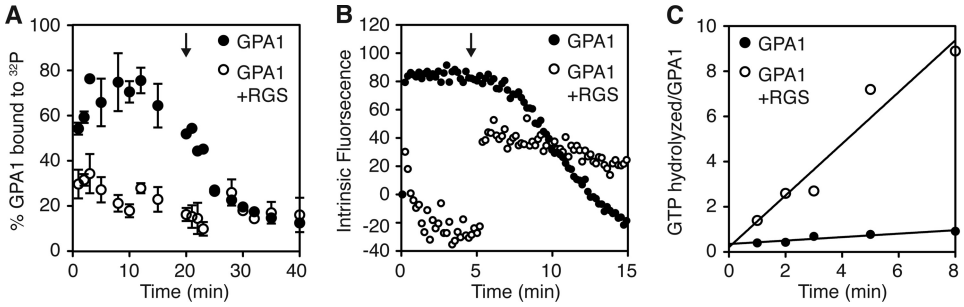

FIGURE 2. **GPA1 activation in the presence of RGS1 protein.** *A*, percent of GPA1 (500 nM) bound to ^{32}P at the given time was measured under steady-state conditions with [γ-^{32}P]GTP (10 μM) and the RGS domain of RGS1 (1 μM) where indicated. Twenty min after starting the reaction, a large excess of GTPγS (100 μM) was added (indicated with an *arrow*) to each sample to prevent further [γ-^{32}P]GTP loading. Data are average and S.E. for four individual experiments. *B*, intrinsic fluorescence (excitation, 284 nm; emission, 340 nm) of GPA1 (300 nM) was measured after the addition of GTP (300 nM) with RGS protein (600 nM) where indicated. Five min after starting the reaction, GTPγS (2 μM) was added to the GPA1+RGS sample (indicated with an *arrow*). Intrinsic fluorescence of GPA1 and RGS protein (where applicable) was subtracted as background prior to the first time point. Data shown for one experiment are representative of three individual experiments. *C*, [γ-^{32}P]GTP hydrolysis by GPA1 (275 nM) was measured with membrane preparations containing full-length RGS1 where indicated. GTPase activity in reactions with RGS1 and GTPase-deficient GPA1^{Q222L} was subtracted as background to account for non-GPA1 GTPase activity in membrane preparations. Data shown for one experiment are representative of three individual experiments.

TABLE 1

Rate of association of guanine nucleotides

Rates are reported as min $^{-1}$.

	MANT-GDP		MANT-GMPPNP		GTPγS
[Mg^{2+}] mM[a]	GPA1	Trimer	GPA1	Trimer	GPA1
0	4.6 (1.0)	2.2 (0.1)	0.89 (0.1)	2.0 (0.3)	0.16 (0.03)
5	6.1 (2.1)	2.6 (0.2)	3.4 (0.7)	2.4 (0.2)	4.1 (0.3)

[a] Concentration of $MgCl_2$ added to buffer containing 1 mM EDTA.

whether AGB1/AGG1 affects Gα activation, we measured rates of Gα binding to MANT-tagged GDP or GMPPNP, a nonhydrolyzable GTP analog. The fluorescence of the MANT group rapidly increases when bound to a Gα protein (26). Like animal Gα proteins, GPA1 association with GDP is unaffected by magnesium in the absence of the G$\beta\gamma$ dimer (Table 1). However, GPA1 association with MANT-GMPPNP is increased from 0.89/min to 3.4/min upon addition of magnesium (Table 1). Magnesium also accelerates GPA1 association with GTPγS, from 0.16/min to 4.1/min (Table 1). When compared with GPA1 alone, the rate of G$\alpha\beta\gamma$ binding to both MANT-GDP and MANT-GMPPNP only is decreased slightly (Table 1). Overall, the effects of the *Arabidopsis* G$\beta\gamma$ dimer on nucleotide exchange are small compared with its mammalian counterparts. These results suggest that GPA1 retains the ability to activate itself even in the presence of the G$\beta\gamma$ dimer.

GPA1 Stabilization by GTP and G$\beta\gamma$ Dimers—Having found only small effects of the G$\beta\gamma$ dimer on GTP binding, we next determined the effect of G$\beta\gamma$ on GTP hydrolysis. GTP hydrolysis can be measured in two ways; steady-state experiments measure sequential rounds of GTP binding and hydrolysis, whereas single turnover experiments measure only one hydrolysis event. We found that each *Arabidopsis* G$\beta\gamma$ dimer (AGB1/AGG1 and AGB1/AGG2) increases the activity of GPA1 in steady-state reactions (Fig. 3*A*) in a dose-dependent manner (Fig. 3*B*). However, the G$\beta\gamma$ dimers do not accelerate single turnover GTP hydrolysis (Fig. 3*C*). Together, these findings suggest that the G$\beta\gamma$ dimer may increase the specific activity of GPA1. In support of this hypothesis, we found that GPA1 specific activity decreases over time with incubation at 23 °C, and the AGB1/AGG1 dimer diminishes this time- and temperature-dependent loss in activity (Fig. 3*D*). GTP also stabilizes GPA1, whereas GPA1 activity diminishes by half after incubation at 23 °C for 1 h with GDP (Fig. 3*D*), and GPA1 activity remains constant over the course of at least 2 h at 23 °C in the presence of GTP (Fig. 3*E*). Together, these results suggest that the unactivated (GDP-bound) form of GPA1 is unstable relative to the activated (GTP-bound) form of GPA1. To test this hypothesis, we measured the thermal stability of GPA1-GDP and GPA1-GTPγS. For this experiment, GPA1 was incubated at a range of temperatures with a fluorescent label that modifies cysteine residues that are exposed to the solvent either by surface location or by protein unfolding (15, 27). We found that the unactivated form of GPA1 is less stable than the activated form of GPA1, with the median melting temperature increasing from 46 °C with GDP to 53 °C with GTPγS (Fig. 3*F*). A similar difference in melting temperatures was observed by circular dichroism (Fig. 4*E*, described below). Together, these data suggest that GPA1 is more stable as a Gα-GTP complex or as a Gα-GDP-G$\beta\gamma$ complex than in complex with GDP alone.

GPA1-GDP Destabilization by N-terminal α-Helix—Our biochemical data show that GPA1 is stabilized by two of its binding partners: GTP and the G$\beta\gamma$ dimer. To identify candidate structural determinants for stabilization of GPA1 by GTP and G$\beta\gamma$, we used all-atom MD simulations to measure motion in GPA1-GTP, GPA1-GDP, and GPA1-GDP-AGB1/AGG1. Toward this end, we constructed a structural model of GPA1-GDP (Fig. 4*A*) using our crystal structure of GPA1-GTPγS (Protein Data Bank code 2XTZ (16)) and Gα_{i1}-GDP (18). The *Arabidopsis* AGB1/AGG1 dimer was modeled essentially as described previously (6). From MD simulations, we found that GPA1-GDP has more dynamic motion than GPA1-GTP, particularly in Switch II and Switch III (Fig. 4*B*). Moreover, monomeric GPA1-GDP has more dynamic motion than GPA1-GDP in the heterotrimeric complex (Fig. 4*C*). This increased motion is found primarily in Switch II and the N-terminal helix, which projects away from the globular part of Gα proteins and contacts the Gβ protein in the heterotrimeric complex (18, 28). Dynamic motion in Switch II is greatly diminished when the N-terminal helix is excluded from the simulation, suggesting that this helix may induce dynamic motion in Switch II (Fig. 4*D*). To determine whether the N-terminal helix contributes to

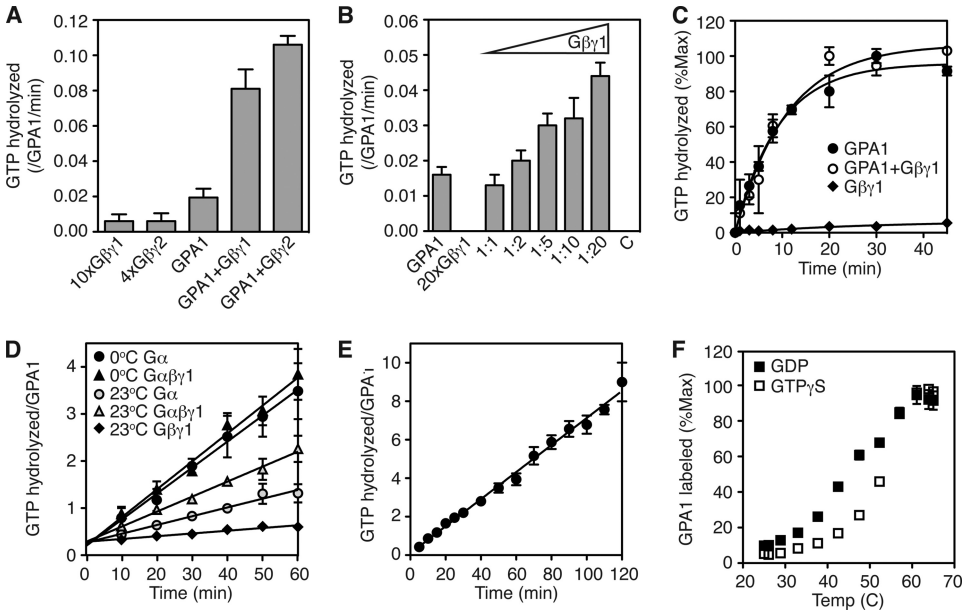

FIGURE 3. **Stabilization of GPA1 by GTP or Gβγ dimers.** *A*, rate of steady-state [γ-^{32}P]GTP hydrolysis by GPA1 (250 nM) with AGB1/AGG1 (Gβγ1, 2.5 μM) or AGB1/AGG2 (Gβγ2, 1 μM) was measured over time. *B*, rate of steady-state [γ-^{32}P]GTP hydrolysis by GPA1 (250 nM) with various concentrations of the AGB1/AGG1 dimer. *C* indicates a control reaction that included GPA1 and a 20-fold molar excess of BSA. *C*, Single turnover [γ-^{32}P]GTP hydrolysis by GPA1 (250 nM) in the presence or absence of AGB1/AGG1 (1250 nM). Data are averages and S.E. for two individual experiments. *D*, steady-state [γ-^{32}P]GTP hydrolysis by purified GPA1 (300 nM) with and without AGB1/AGG1 (2500 nM) was measured over time after incubation on ice (0 °C) or at room temperature (23 °C). Data are averages and S.E. for two individual experiments. *E*, steady-state [γ-^{32}P]GTP hydrolysis by purified GPA1 (300 nM). Data are averages and S.E. for three individual experiments. *F*, GPA1 unfolding was quantified by measuring fluorescent labeling of exposed cysteine residues (excitation, 400 nm; emission, 500 nm) over a range of temperatures after incubation with GDP or GTPγS (33 μM). Shown are the averages and S.E. for four experiments.

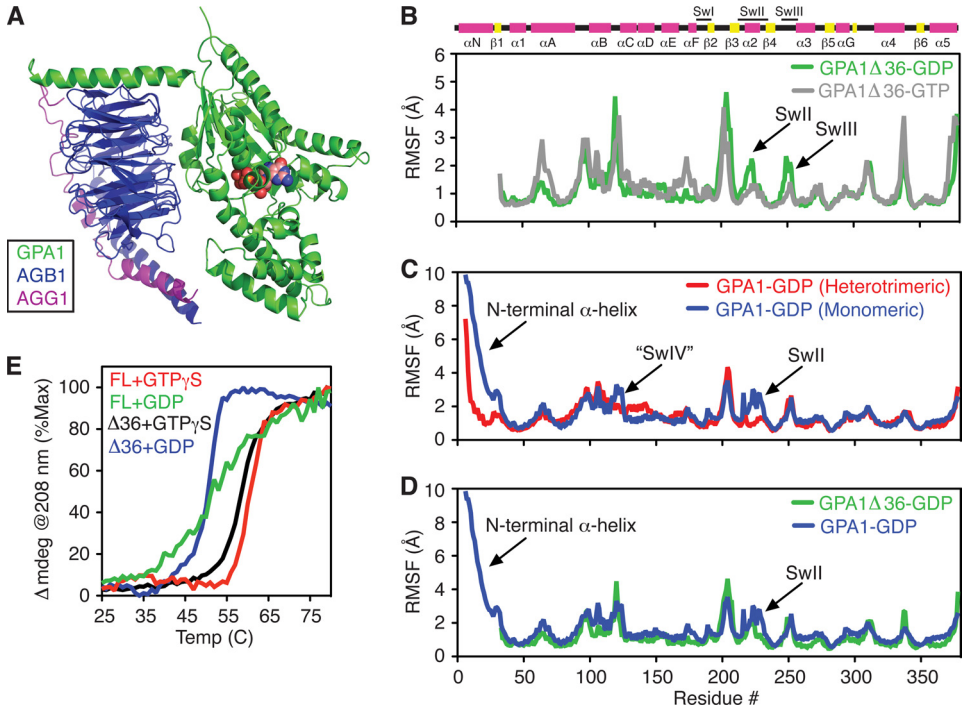

FIGURE 4. **Molecular dynamics simulations with GPA1.** *A*, structural model of GPA1-GDP (residues 10–383, *green*) in complex with AGB1 (residues 8–369, *blue*) and AGG1 (residues 26–80, *magenta*) generated from homologous structures. *B*, root mean square fluctuation about an average structure for each residue in GPA1Δ36-GDP (*green*) or GPA1Δ36-GTP (*gray*) calculated from MD simulations. *C*, root mean square fluctuations for GPA1-GDP (*blue*) or GPA1-GDP-AGB1/AGG1 (*red*). *D*, root mean square fluctuations for full-length GPA1-GDP (*blue*) or GPA1Δ36-GDP (*green*). *E*, temperature-induced unfolding of Gα proteins monitored by circular dichroism at 208 nm. *FL*, full-length GPA1; Δ36, GPA1 with the N-terminal 36 residues deleted; *SwII*, Switch II; *SwIII*, Switch III; "*SwIV*", postulated switch IV; *Temp*, temperature.

the reduced stability of GPA1-GDP relative to GPA1-GTPγS, we measured the secondary structure content of GPA1 as a function of temperature. Like the full-length protein, we found that GPA1 lacking the first 36 amino acids (GPA1Δ36) is less stable in complex with GDP than with GTPγS (Fig. 4*E*). The Δ36 deletion does not affect the stability of the Gα-GTPγS

complex. However, removing the N-terminal helix stabilizes GPA1-GDP at temperatures below 45 °C and increases the cooperativity of the unfolding transition relative to the full-length protein (Fig. 4*E*). Together, these results suggest that the dynamic motion in the free N-terminal helix and switch regions of GPA1 contribute to the instability of this protein that we observed in the absence of the G$\beta\gamma$ dimer. More broadly, our findings show that the G$\beta\gamma$ dimers and RGS1 cooperate to maintain an unactivated but fully functional pool of GPA1.

DISCUSSION

During the past several decades, G protein signaling in animals has been characterized extensively at the physiological, pharmacological, cellular, genetic, biochemical, and molecular level. Investigations of G protein signaling in plants have been far more limited, but these studies have revealed at least three major differences from the animal system. First, the *Arabidopsis* Gα protein has unusual activation kinetics; GPA1 can activate itself without a GPCR or other guanine nucleotide exchange factor (5). Second, the *Arabidopsis* RGS1 protein has an atypical domain architecture, comprised of a receptor-like domain fused to an RGS domain (7). Third, GPA1 is reported to exist primarily in the monomeric state *in vivo* (13). Taken together, these findings suggest that GPA1 may exist permanently in the dissociated and GTP-bound state, perhaps the consequence of persistent self-activation. Given these unique properties, we regard the *Arabidopsis* system as an instructive counterexample to the well established signaling paradigm in animals.

Here, we purified and reconstituted GPA1 with its binding partners, the G$\beta\gamma$ subunits and the full-length RGS1 membrane protein. Our data reveal how these factors regulate GPA1 activity. First, we show for the first time that the full-length RGS1 protein accelerates GTPase activity. These findings are significant because they reveal that no ligand is required for RGS1 GTPase-accelerating activity, despite the presence of a GPCR-like domain (see below). Furthermore, we show for the first time that GPA1 can bind to the presumed G$\beta\gamma$ subunits directly, and these proteins assemble in a nucleotide-dependent manner. Although animal G$\beta\gamma$ dimers are well known to diminish basal G protein activation, we found that the plant Gα protein retains the fast nucleotide exchange property in the presence of the G$\beta\gamma$ dimer. Moreover, similar to mammalian Gα proteins (29), GPA1-GDP is unstable relative to Gα-GTPγS, and G$\beta\gamma$ dimers stabilize GPA1-GDP. Finally, we found that the N-terminal helix destabilizes GPA1 in the absence of the G$\beta\gamma$ dimer.

Molecular dynamics simulations were critical to our analyses of GPA1 stability. Although crystal structures provide a "snapshot" of a single protein conformation, molecular dynamics simulations build upon the information in crystal structures to reveal dynamic motion in proteins. Our simulations led to the hypothesis that the N-terminal α-helix of GPA1 affects the stability of the unactivated Gα-GDP complex by destabilizing Switch II. This hypothesis was supported in biophysical measurement of protein stability by circular dichroism.

Our studies resolve a seeming paradox in plant G protein signaling. How can GPA1 have an extremely fast spontaneous rate of nucleotide exchange, yet not be constitutively active and entirely monomeric *in vivo*? Consistent with the earlier finding that much of GPA1 is monomeric in plants (13), we found that purified GPA1 is predominantly activated in the presence of excess GTP. However, RGS1 reduces the fraction of activated GPA1 and therefore would promote heterotrimer association in a cell. Moreover, cell-based fluorescence studies suggested that a constitutively active form of GPA1 (Q222L, abolishes GTPase activity) remains in the heterotrimer state in cowpea protoplasts (1). These *in vivo* results, although unexpected, can be reconciled with our *in vitro* data showing that Gα-GTPγS binding disrupts the heterotrimeric complex. Indeed GPA1 and AGB1 may remain associated as a part of a large macromolecular complex in cells (13), or the subunits may dissociate but remain in sufficiently close proximity at the plasma membrane to elicit an interaction signal. We have shown that purified GPA1 exists largely in the GTP-bound state without RGS1. If cowpea protoplasts lack RGS1-like activity, GPA1 and GPA1^{Q222L} should behave similarly with respect to G$\beta\gamma$ association as reported (1).

Another question is whether RGS1 regulates signaling in a dynamic manner. The presence of a GPCR-like domain suggests that the protein may respond to a ligand that in turn alters GPA1 activity in the cell. Our findings indicate that full-length RGS1 accelerates GTPase activity in the absence of any stimulus. Thus, the receptor-like domain may serve simply to anchor the RGS domain to the plasma membrane. Alternatively, a ligand may exist that modulates, but does not initiate, GTPase-accelerating activity. The possibility that the GAP activity of this protein is regulated by ligand binding to the receptor domain remains to be determined. D-glucose (or a sugar metabolite) is a candidate regulatory ligand for RGS1 (5, 30). However, our efforts to detect glucose-dependent changes in GAP activity have thus far been inconclusive.

Together, our results show that the *Arabidopsis* heterotrimer and RGS protein have properties similar to their animal counterparts, despite the self-activation property of GPA1 and the atypical domain architecture of RGS1. Similar to that in animals, heterotrimeric components from plants only associate in the presence of GDP, and GTP disrupts the heterotrimer. Indeed, many of the residues that confer basic Gα functions (GTP binding, GTP hydrolysis, G$\beta\gamma$ binding) are nearly invariant between plant and animal G proteins. Thus, our findings further support the hypothesis that the structural determinants that govern heterotrimer association were established in a common ancestor of plants, animals, and fungi (31).

Acknowledgments—We are grateful to Janeen Vanhooke, Adam Kimple, and Tyrell Carr for providing proteins used in this study; John Sondek for sharing equipment; and Dan Isom for sharing expertise.

REFERENCES

1. Adjobo-Hermans, M. J., Goedhart, J., and Gadella, T. W., Jr. (2006) *J. Cell. Sci.* **119,** 5087–5097
2. Digby, G. J., Lober, R. M., Sethi, P. R., and Lambert, N. A. (2006) *Proc. Natl. Acad. Sci. U.S.A.* **103,** 17789–17794
3. Gilman, A. G. (1987) *Annu. Rev. Biochem.* **56,** 615–649
4. Dohlman, H. G., Thorner, J., Caron, M. G., and Lefkowitz, R. J. (1991)

Annu. Rev. Biochem. **60,** 653–688
5. Johnston, C. A., Taylor, J. P., Gao, Y., Kimple, A. J., Grigston, J. C., Chen, J. G., Siderovski, D. P., Jones, A. M., and Willard, F. S. (2007) *Proc. Natl. Acad. Sci. U.S.A.* **104,** 17317–17322
6. Ullah, H., Chen, J. G., Temple, B., Boyes, D. C., Alonso, J. M., Davis, K. R., Ecker, J. R., and Jones, A. M. (2003) *Plant Cell.* **15,** 393–409
7. Chen, J. G., Willard, F. S., Huang, J., Liang, J., Chasse, S. A., Jones, A. M., and Siderovski, D. P. (2003) *Science* **301,** 1728–1731
8. Higashijima, T., Ferguson, K. M., Sternweis, P. C., Smigel, M. D., and Gilman, A. G. (1987) *J. Biol. Chem.* **262,** 762–766
9. Weiss, C. A., Garnaat, C. W., Mukai, K., Hu, Y., and Ma, H. (1994) *Proc. Natl. Acad. Sci. U.S.A.* **91,** 9554–9558
10. Trusov, Y., Zhang, W., Assmann, S. M., and Botella, J. R. (2008) *Plant Physiol.* **147,** 636–649
11. Mason, M. G., and Botella, J. R. (2001) *Biochim. Biophys. Acta.* **1520,** 147–153
12. Mason, M. G., and Botella, J. R. (2000) *Proc. Natl. Acad. Sci. U.S.A.* **97,** 14784–14788
13. Wang, S., Assmann, S. M., and Fedoroff, N. V. (2008) *J. Biol. Chem.* **283,** 13913–13922
14. Willard, F. S., and Siderovski, D. P. (2004) *Methods Enzymol.* **389,** 320–338
15. Isom, D. G., Marguet, P. R., Oas, T. G., and Hellinga, H. W. (2010) *Proteins* DOI: 10.1002/prot.22932
16. Jones, J. C., Duffy, J. W., Machius, M., Temple, B. R., Dohlman, H. G., and Jones, A. M. (2011) *Sci. Signal.* **4,** ra8
17. Eswar, N., Webb, B., Marti-Renom, M. A., Madhusudhan, M. S., Eramian, D., Shen, M. Y., Pieper, U., and Sali, A. (2006) *Current Protocols in Bioinformatics* DOI: 10.1002/0471250953.bi0506s15
18. Wall, M. A., Coleman, D. E., Lee, E., Iñiguez-Lluhi, J. A., Posner, B. A., Gilman, A. G., and Sprang, S. R. (1995) *Cell* **83,** 1047–1058
19. Teotico, D. G., Frazier, M. L., Ding, F., Dokholyan, N. V., Temple, B. R., and Redinbo, M. R. (2008) *PLoS. Comput. Biol.* **4,** e1000111
20. Ryan, M. M., Temple, B. R., Phillips, S. E., and Bankaitis, V. A. (2007) *Mol. Biol. Cell.* **18,** 1928–1942
21. Duan, Y., Wu, C., Chowdhury, S., Lee, M. C., Xiong, G., Zhang, W., Yang, R., Cieplak, P., Luo, R., Lee, T., Caldwell, J., Wang, J., and Kollman, P. (2003) *J. Comput. Chem.* **24,** 1999–2012
22. Tesmer, J. J., Berman, D. M., Gilman, A. G., and Sprang, S. R. (1997) *Cell* **89,** 251–261
23. Berman, D. M., Wilkie, T. M., and Gilman, A. G. (1996) *Cell* **86,** 445–452
24. Higashijima, T., Ferguson, K. M., Sternweis, P. C., Ross, E. M., Smigel, M. D., and Gilman, A. G. (1987) *J. Biol. Chem.* **262,** 752–756
25. Higashijima, T., Ferguson, K. M., Smigel, M. D., and Gilman, A. G. (1987) *J. Biol. Chem.* **262,** 757–761
26. Neal, S. E., Eccleston, J. F., and Webb, M. R. (1990) *Proc. Natl. Acad. Sci. U.S.A.* **87,** 3562–3565
27. Isom, D. G., Vardy, E., Oas, T. G., and Hellinga, H. W. *Proc. Natl. Acad. Sci. U.S.A.* **107,** 4908–4913
28. Lambright, D. G., Sondek, J., Bohm, A., Skiba, N. P., Hamm, H. E., and Sigler, P. B. (1996) *Nature* **379,** 311–319
29. Posner, B. A., Mixon, M. B., Wall, M. A., Sprang, S. R., and Gilman, A. G. (1998) *J. Biol. Chem.* **273,** 21752–21758
30. Chen, J. G., and Jones, A. M. (2004) *Methods Enzymol.* **389,** 338–350
31. Temple, B. R., Jones, C. D., and Jones, A. M. (2010) *PLOS Comput.* **6,** e1000962